A Non-conventional Durability Test for Simulating Creep of Geosynthetics Under Accelerated Degradation

José Luiz Ernandes Dias Filho[1] · Paulo Cesar de Almeida Maia[1]

Abstract

The evaluation of the durability of geosynthetics for application in real structures is an important field of investigation. Within this field, the interaction between degradation agents that geosynthetics can be subject to, in their different applications, is an increasingly studied issue, because it can have direct implications in the design of the materials. Thus, this article explores a non-conventional test for geosynthetics, to simulate creep under accelerated conditions using a saturation and drying procedure simultaneous to the creep process. In this way, the material is closer to the exogenous field conditions as in, for example, riverside projects or even in coastal protection. For this, a total of 48 tests of conventional creep and under accelerated degradation conditions were carried out in 4 different geotextiles. From these tests, models were proposed and presented coefficients of determination greater than 0.84. Additional results indicate an increased strain rate ranging between 5 and 16 times in creep test from the moment that degradation simultaneous with creep is induced. Reduction factors greater than 3 indicated a very aggressive degradation process. In general, the study showed that ensuring the design life of geosynthetics calls for a simulation of degradation conditions that demand more from these materials. By enabling a more precise analysis of field conditions the creep test under accelerated conditions presents an excellent tool for project design. The significance of this study for geosynthetics design is in providing general knowledge of creep under accelerated conditions using equations and models to determine important geosynthetic parameters.

Keywords Geosynthetics · Geotextiles · Durability · Degradation · Creep

Introduction

Behavior characterization tests are widely used for all construction materials, providing essential data for the design and development of engineering projects. Technological advances have enabled the development of increasingly refined and accurate testing techniques. However, such tests are usually subject to limitations, especially related to stress–strain state and boundary conditions, which, in some cases, may not represent field conditions. This is relevant in the case of geosynthetics, given the complexity of modelling the intrinsic characteristics of the constituent materials, the geometry and the interaction with the soil. The long-term behavior of these materials is even more complex, which has led the scientific community to search for more representative procedures to simulate the behavior of these materials.

Geosynthetics are widely used in engineering across many types of projects around the world. The variety of regional conditions in the application of these materials means that there will be different degradation mechanisms acting. Understanding the exogenous environment and the degradation agents is fundamental to choosing the best form of characterization test to apply [1–5].

Solutions using sand-filled geosynthetic tubes, for example, are prominent in projects that aim to minimize the impact of surface dynamics processes. The main projects with these characteristics dated to the 1950s [6, 7]. Studies by Restall et al. [8] and Hornsey et al. [9] present damage from a common form of drilling in hydraulic projects, either through small holes generated by unintended sharp elements, or by the occurrence of knife cuts. The technical literature also presents problems related to the durability of

✉ José Luiz Ernandes Dias Filho
 jlernandes@hotmail.com

 Paulo Cesar de Almeida Maia
 maia@uenf.br

[1] Civil Engineering Laboratory, Darcy Ribeiro State University of Northern Rio de Janeiro, Campos, RJ 28013-602, Brazil

structures with tubular textile forms compromised by rupture, displacement, damage and clogging [10–12]. Research has highlighted the need for more studies on soil–geotextile interaction to obtain better solutions for stresses and deformation behavior [13, 14], as well as installation damage [15–17]. Elias et al. [18] and Tan et al. [19] describe natural elements as stress concentrators. For all of these cases, the thickness of the geosynthetics is important to prevent perforation.

Considering the observations above, this type of demand on the geosynthetic is negligible, since with proper design, increasing thickness is a practice that minimizes the effects of perforation. In another example, as reported by Koerner et al. [20], the addition of a second geosynthetic layer for protection is a viable solution for materials without ultraviolet radiation protection. Thus, important variables in the design of geosynthetic tubular structures for river and coastal protection conditions, such as exposure to radiation and perforation, make clear the need for analyses that involve, for example, saturation-drying cycles in the exposed environment [21–23], as well as the analysis of creep deformations [15, 24–27].

Because of the importance of durability properties in geosynthetics design, this paper explores a non-conventional approach to evaluating long-term behavior by taking into consideration creep under accelerated degradation conditions. The flowchart in Fig. 1 compares the five phases involved in predicting long-term behavior under both the conventional and non-conventional approaches. The first phase is to obtain the study material. This is followed by the production of samples either with accelerated degradation induced in the laboratory or with natural weathering in the field. After the degradation of the samples, the properties that define the characteristic behavior of the material are determined: physical, mechanical, hydraulic or performance. Then the related parameters that characterize the properties of intact and degraded materials are obtained (except for the material from non-conventional test that was used for the determination of the characteristic behaviors during the degradation process—phases 2 and 3 together). Finally, the results are analyzed and the long-term behavior of the material is predicted.

The established and standardized methods for durability tests, referred to here as conventional, are the international references ISO/TS 13434 [28] and ASTM D5970 [29]. They address durability testing by presenting the necessary procedures for conventional testing methods. However, according to Suits and Hsuan [1], these conventional methods can be accelerated with special procedures. The ASTM G90 [30] describes standard practice for accelerated outdoor weathering of non-metallic materials from natural sunlight using concentrator equipment. The methods for accelerated degradation in the laboratory are specified in both ASTM D5819 [31] and ISO/TS 13434 [28]. For degradation procedures, these methods provide a faster variation in the properties of materials that are subject to some specific type of alterability or synergy, in a shorter time period. Among them are biological degradation, chemical degradation, creep by conventional or the SIM method (Stepped Isothermal Method), mechanical damage, abrasion, photodegradation and thermal
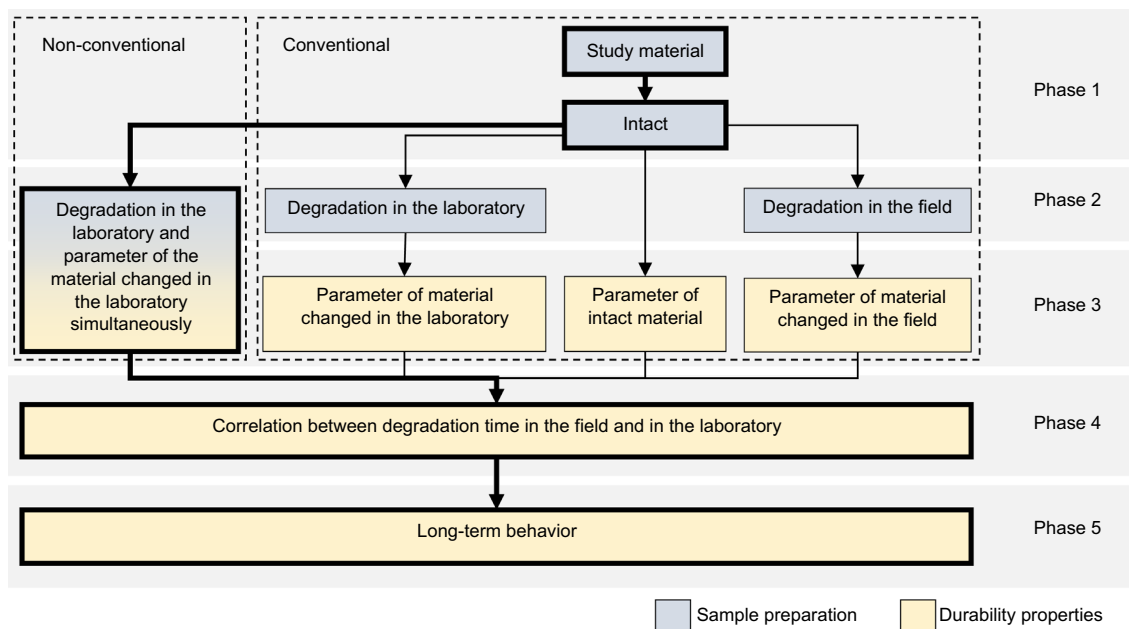

Fig. 1 Methodologies in projects to predict the long-term behavior of geosynthetics

degradation. It is important to highlight that there is a protocol for the execution and analysis of the results for each laboratory procedure, based on the principal degradation mechanisms related to the application of geosynthetics in engineering projects.

Based on established methods, some researchers have analyzed the interaction of more than one standardized procedure for assessing durability. These methods analyze the synergy of the exposure of geosynthetics to more than one degradation mechanism. There are numerous combinations of degradation mechanisms and some examples of this research include studies with thermal oxidation and ultraviolet radiation [4, 5, 32], natural exposure and immersion in acids at different temperatures [33, 34], with creep and natural exposure [27], installation damage [17] or immersion in acid and base solutions [35].

The choice of method varies according to the application of the geosynthetic in a project, which is typically subject to more than one degradation mechanism. The specific situations studied by the authors cited above generated the demand for tests and enabled a better understanding of the extent to which synergy contributes to studies on the durability of materials. It is important to highlight that in the design of structures that use geosynthetics, their long-term behavior may be evaluated by taking into consideration the effects of installation damage, creep and durability.

This present study was intended to simulate some degradation conditions related to riverside and coastal protection projects (tubular structures, erosion control, etc.). Therefore, a novel test apparatus was developed to perform laboratory experiments, enabling the execution of up to 16 simultaneous creep tests under combinations of degradation conditions involving temperature, water and ventilation. The new testing device was designed to perform creep tests under specific degradation conditions, facilitating evaluation of the deformation parameters of the materials simultaneously with the induced degradation process. This non-conventional approach enables long-term behavior studies that more closely approximate real-world application conditions, taking into consideration various degradation agents and permitting greater control of the variables involved with these processes.

Recent published studies have examined interactions between degradation agents, however, without considering the combined effect of creep and accelerated degradation through saturation-drying cycles. Therefore, this study aimed to contribute to the understanding of problems in the application of geotextiles in structures subject to surface dynamics conditions. Evaluation of the synergy between creep and accelerated degradation conditions was done by employing saturation and drying cycles in four geotextiles to simulate more realistic field conditions for tubular textile structures.

Materials and Methods

Study Material

Table 1 shows reference values for the nominal characteristics of the four woven geotextiles of different weights, which are presented in Fig. 2, that were chosen for the testing program. Two tests were carried out on multifilament polyester (PET) and two on monofilament polypropylene (PP). The samples were cut in the machine direction (MD), and the stress–strain behavior of the virgin sample was determined using the wide-width strip method test according to ASTM D5035-11 [36]. Physical index tests were conducted according to the standards for determining mass per unit area [37] and nominal thickness [38].

The tensile tests were conducted in a universal testing machine, 23 EMIC with 30 kN capacity and a load cell of 10 kN, in the laboratory with internal temperature controlled at 20 ± 2 °C and relative humidity of $65 \pm 5\%$. The width of the test specimens was 50 ± 5 mm and length of 100 mm between clamps. The elongation was measured by video-extensometer at a constant rate of deformation of 10%/min of the gauge length.
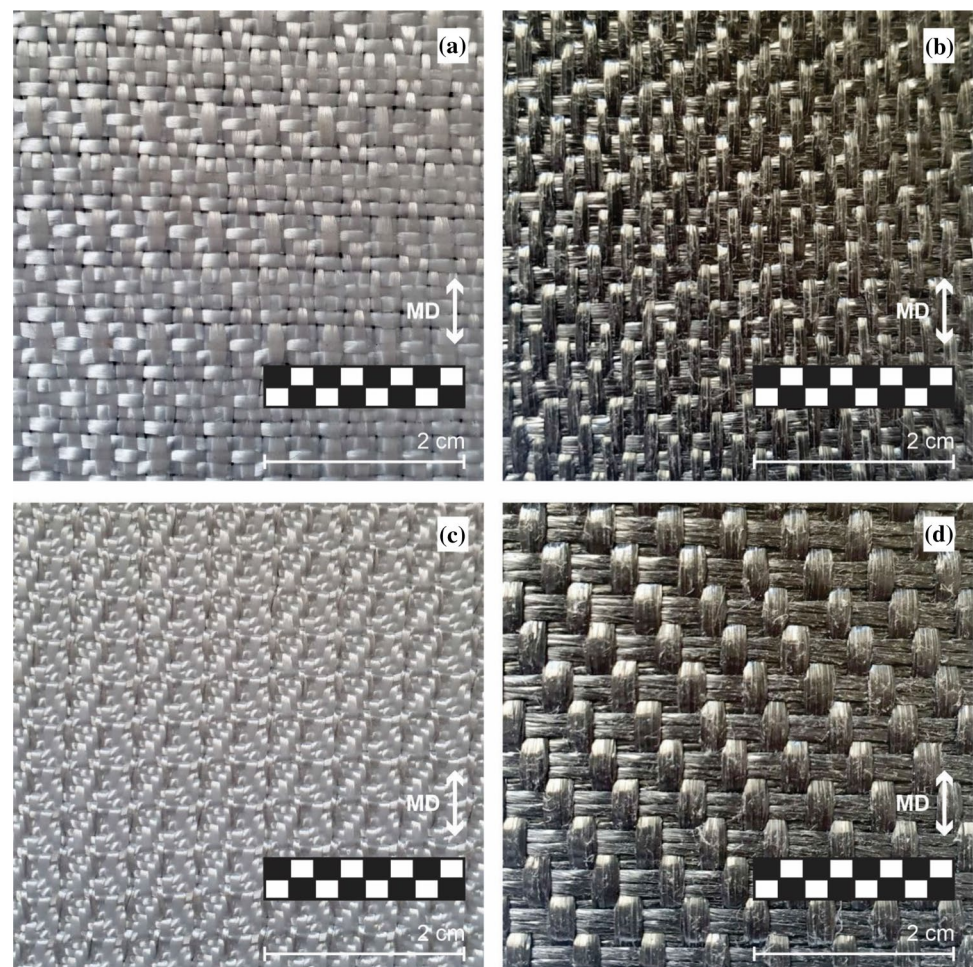
Test Procedure

This research used two test procedures to better understand the extent to which synergy contributes to studies of the durability of the materials. For the proposed non-conventional procedure, we seek to determine the mechanical and durability characteristics of the geotextiles by means of the synergy between creep and accelerated degradation through saturation and drying cycles. The methodology for the development of the study is illustrated in the flowchart

Table 1 Reference values for the nominal characteristics of the woven geotextiles

Property	Test standard	PET340	PP500	PET740	PP925
Ultimate tensile strength (kN/m)	[36]	52.5 ± 1.6	106.2 ± 2.0	150.7 ± 5.2	155 ± 1.6
Elongation at rupture (%)	[36]	16.5 ± 1.8	20.1 ± 1.3	34.8 ± 1.8	28.5 ± 2.1
Mass per unit area (g/m²)	[37]	340 ± 8	500 ± 9	740 ± 23	925 ± 25
Thickness (mm)	[38]	0.51 ± 0.02	1.53 ± 0.04	1.17 ± 0.01	2.62 ± 0.06

Fig. 2 Visual characteristics of the four geotextiles in the study: **a** PET340; **b** PP500; **c** PET740; **d** PP925

in Fig. 1. The path highlighted in the chart represents the non-conventional approach used for this study.

This research differs from previous studies in its use of the degradation procedure simultaneously with the creep test to obtain test parameters in an accelerated way. As mentioned in the Introduction, the combination of phases 2 and 3 used in this methodology reduce the time needed to perform durability studies by eliminating the need to obtain parameters after first subjecting samples to degradation procedures in the field and/or laboratory.

The testing program consisted of determining the creep deformation behavior for loads of 10%, 20%, 30% and 40% of the rupture load according to the testing standards [39] for the four woven geotextile samples. That is to say 16 conventional tests, as well as 32 non-conventional creep tests under simultaneous degradation, or a total of 48 tests. For this, the 16 conventional tests were conducted in the laboratory with a controlled internal temperature of 20 ± 2 °C and relative humidity of $65 \pm 5\%$ for a period of up to 10,080 h, and up to 336 h for the creep tests with simultaneous degradation. The specimens were 50 ± 5 mm wide and length of 50 mm between clamps. The elongation

was measured by dial indicator connected to the clamps by tell tales.

The first 16 accelerated tests began in the same way as the conventional ones, i.e., until 24 h had passed and the saturation and drying equipment was turned on for the first battery of tests. The other 16 accelerated tests consisted of carrying out the same tests by turning on the equipment after 12 h.

Isochronous creep curves, obtained using the model equation from Dias Filho et al. [40] for representation of strain–time relationships, were calculated with the test results for all samples and load levels, according to Eq. 1:

$$\varepsilon = cT^{d} \ln(t) + eT. \tag{1}$$

It is possible to calculate the behavior of the strain ε (%), over time t (days). Parameter c is a coefficient which correlates the deformation with the load level T (kN/m) raised to the power d (%/T^{d}) and the slope coefficient e, which correlates the deformation with the load level (%/kN/m). According to Dias Filho et al. [40] the first portion of the equation is a potential function and the second part is linear, which produces a good representation of the behavior of the

creep tests, where the inclination of the curves gradually changes with the increase in the load applied to the test sample. When the time varies between 0 and 1, the data range is not excluded, the second part of equation corrects the data according to the applied load.

Particularly for the accelerated test, the equation only applies for times greater than 12 or 24 h depending on the time the equipment was turned on. The method allows for extrapolation of test data to obtain deformations over time, even for load levels different from the values applied in the tests. This study was primarily concerned with the use of geotextile and can be applied to geogrids as well.

Equipment

The analysis of the samples using the accelerated degradation procedure in the laboratory and simultaneously obtaining the parameter of the material altered was performed using equipment specially built for research at the Durability Testing Laboratory—GeoLED, which is part of the Civil Engineering Laboratory at Darcy Ribeiro State University of Northern Rio de Janeiro—UENF.

The laboratory's saturation and drying equipment (Fig. 3) was adapted with components for the special creep tests, as shown in Fig. 4. The first adaptation was a rigid base with 32 dial indicators attached to four panels to measure the displacements for the 16 simultaneous tests and the cover (Fig. 4a). The cover was produced in such a way that it was possible to insert the rods necessary to carry out the specimen deformation measurements. The control panel in Fig. 4b shows the time, saturation, drying and ventilation counters, and the temperature displays

corresponding to the two thermocouples inside the tank. This control panel is used to set the cycles and temperature limits, for the test to automatically happen under controlled conditions. Below the control panel are two pumps. The first one, with white hoses, is responsible for suctioning water from the water tank and directing it to the tank for saturation of the specimens. The second, with blue hoses, drains the storage tank in Fig. 4c.

After the saturation process in the tank, the drying cycle begins. At this time, the heat resistor is switched on and remains so for the established time. The next step is to cool the tank with ventilation so that there is no thermal shock between the cycles (Fig. 4d). After the established time, the tank saturation process is resumed. In summary, the following times were established: 120 min of saturation of the specimens with water at room temperature, 120 min of drying with a maximum temperature of 70 °C and 20 min of ventilation. The total time of the test cycle also includes an additional 20 min, of which 8 min are needed to fill the tank and 12 min to empty. The saturation and drying equipment complete a cycle with a total time of 280 min.

The saturation and drying times were based on tests evaluating the saturated and dry weight of samples of the geotextiles studied over time. Measurements of the weight in the test samples were taken at preset times of 1, 2, 4, 8, 15, 30 and 60 min, then at 2, 4, 8 and 24 h. Thus, samples dried in an oven for 24 h were immersed in water and, at the recommended time intervals, were weighed and returned to immersion after reading their weight. On the other hand, other samples of geotextiles saturated for 24 h were submitted to drying in an oven and, at the recommended time intervals, they were weighed and returned to the oven after
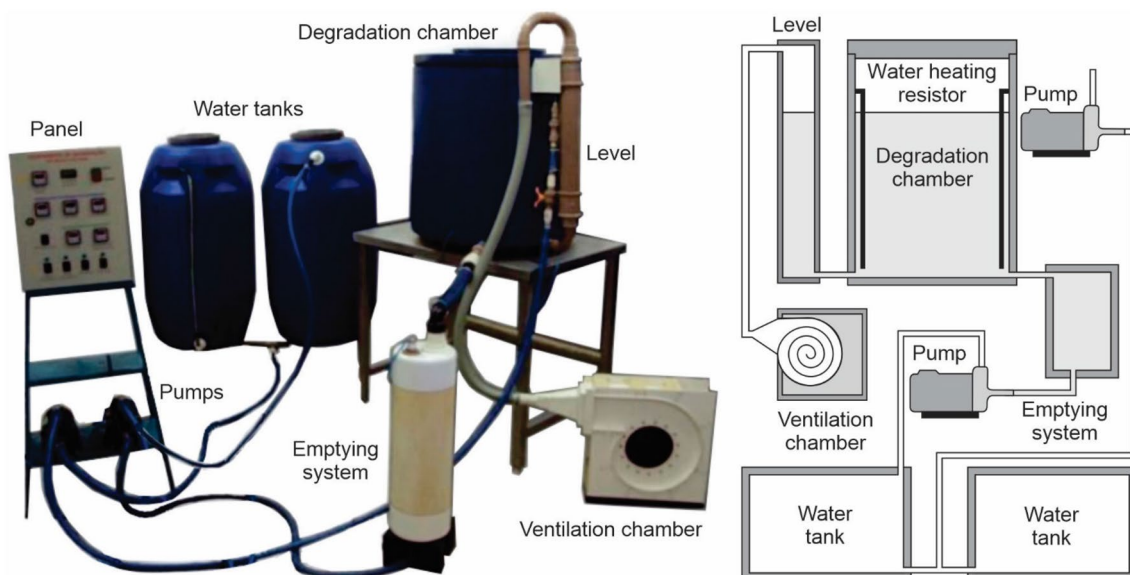

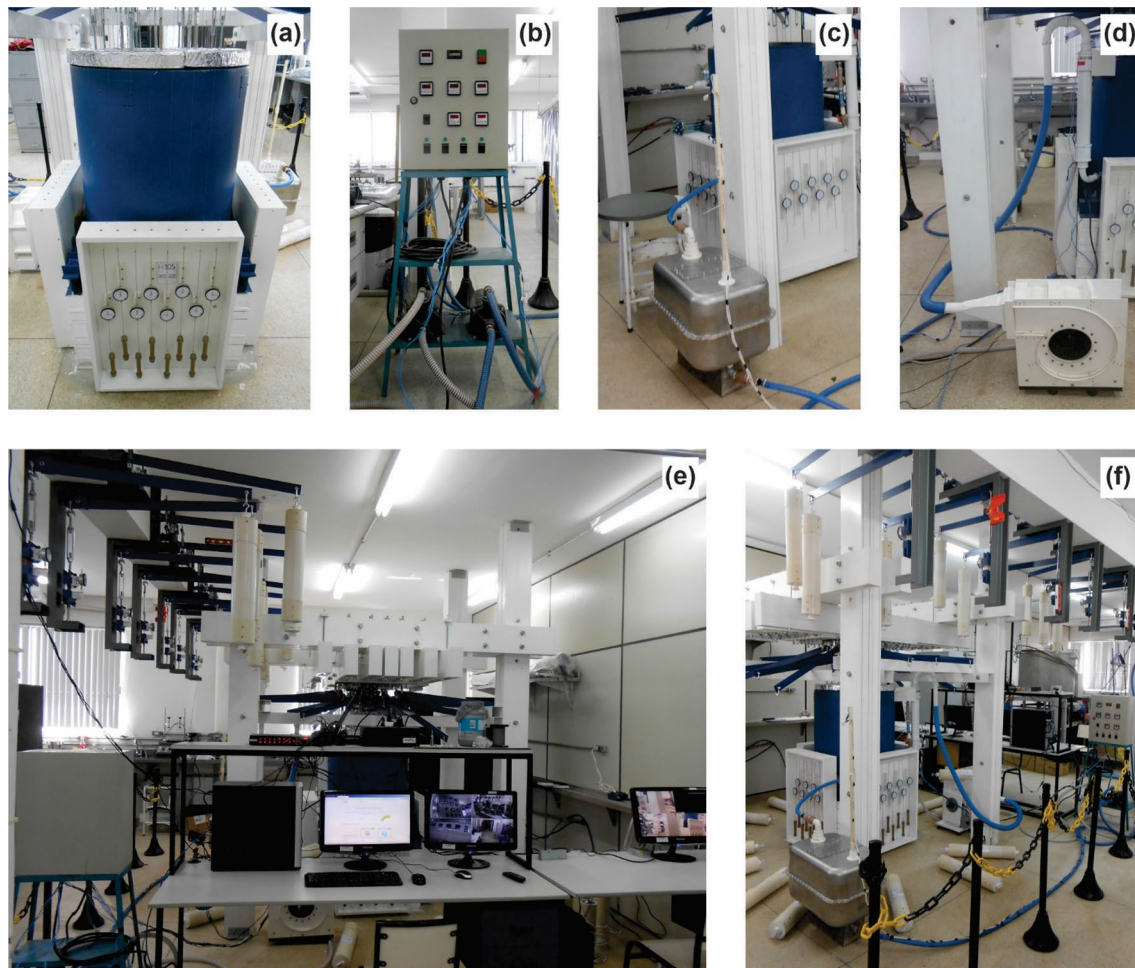**Fig. 3** Schematic and automatic saturation and drying equipment at UENF

Fig. 4 Equipment for creep test with simultaneous degradation: **a** degradation chamber and dial indicators; **b** panel; **c** emptying system; **d** ventilation chamber; **e** monitoring; **f** general overview

reading their weight. Two hours were enough to reach with 95% confidence the saturated or dry weight of the samples.

The test temperature was based on the work of Prellwitz et al. [23], which evaluated the degradation of geotextiles by saturation-drying cycles. The difference between the strength results obtained between samples under drying conditions at 75 °C and 100 °C was negligible. Therefore, to optimize the operation of the equipment, drying was set at approximately 70 °C. Under these conditions, it is possible to obtain parameters of degraded geotextiles in a short period of time, evaluate the results and propose better correlations of the study parameters for field applications. It is important to highlight that temperature variation and water contact are predominant situations in riverside and coastal protection projects.

Figure 4e shows the monitoring system, which records the images from the cameras positioned in front of the dial indicators panels. The images were recorded to acquire

data at any time during the test and to record movement around the equipment and Fig. 4f is a general overview of the complete structure for the test. Figure 5 shows the calibration of the saturation and drying chamber with the temperature variation over several hours during the saturation and drying cycles to guarantee the imposed limits. The entire process was monitored, allowing the temperature to be monitored over time and its behavior with little variation until the end of the tests, which ended in 72 cycles.

Figure 6 shows a schematic drawing of the system for measuring the displacements between the clamps of the top and bottom of the test specimens, which are inside the degradation chamber of the saturation and drying equipment. This system consists of plates screwed tightly around the sample. The steel rods at each end contain the communication system with the dial indicators by tell tales, which are part of the peripherals needed for execution and data collection.
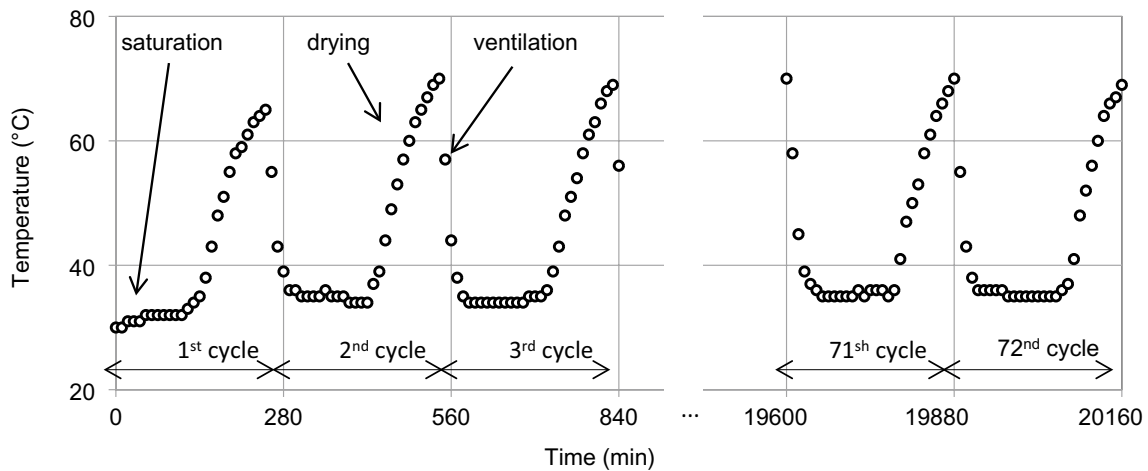
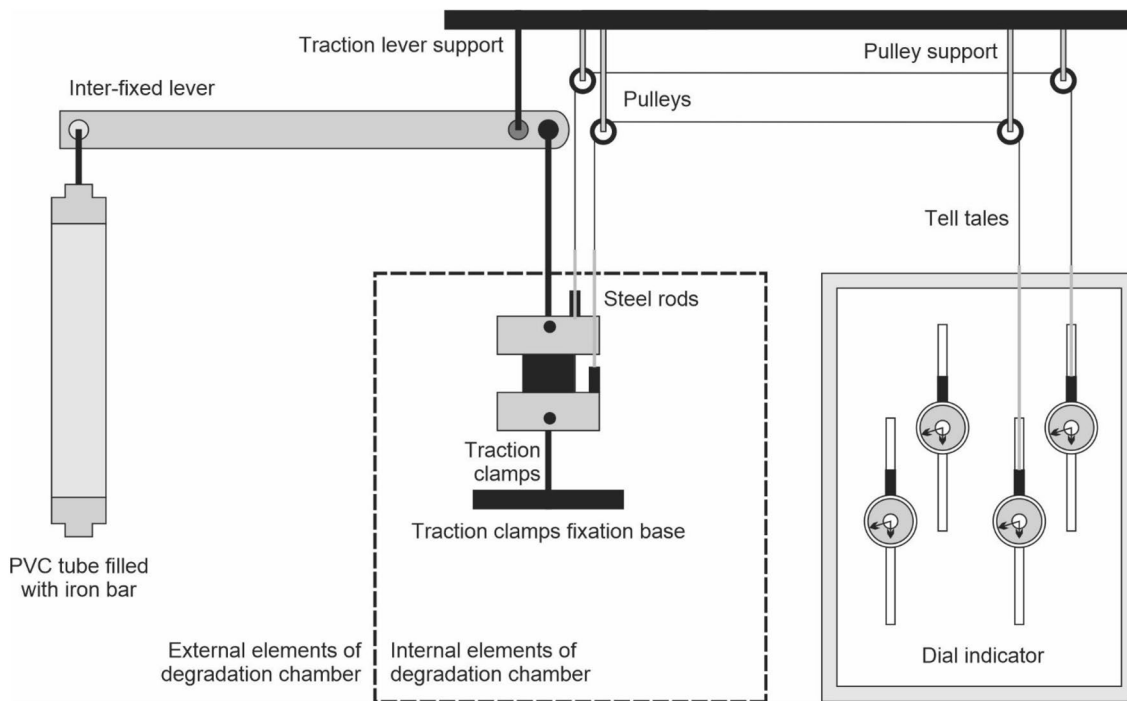**Fig. 5** Calibration of the saturation and drying chamber

Fig. 6 Schematic of the creep test with simultaneous degradation

Results and Discussion

Figure 7 shows the results of the battery of creep deformation tests, 12 per material tested, completed in up to 14 days or 336 h. It presents the conventional creep tests and the non-conventional creep test with simultaneous degradation. Thus, each graph in Fig. 7 contains 3 creep test results by loading level, one as a conventional test, one under accelerated degradation after 24 h and the other under accelerated degradation after 12 h. The boundary between the two phases of creep in the figure was defined according to the first portion of the equation, that is, the moment at which the tangent of the creep became constant, which occurred after 8 h of testing.

As can be seen in the figure, the deformations are directly proportional to the variation in the test time during the primary creep stage. In the secondary stage there is strong evidence of the effect of simultaneous accelerated
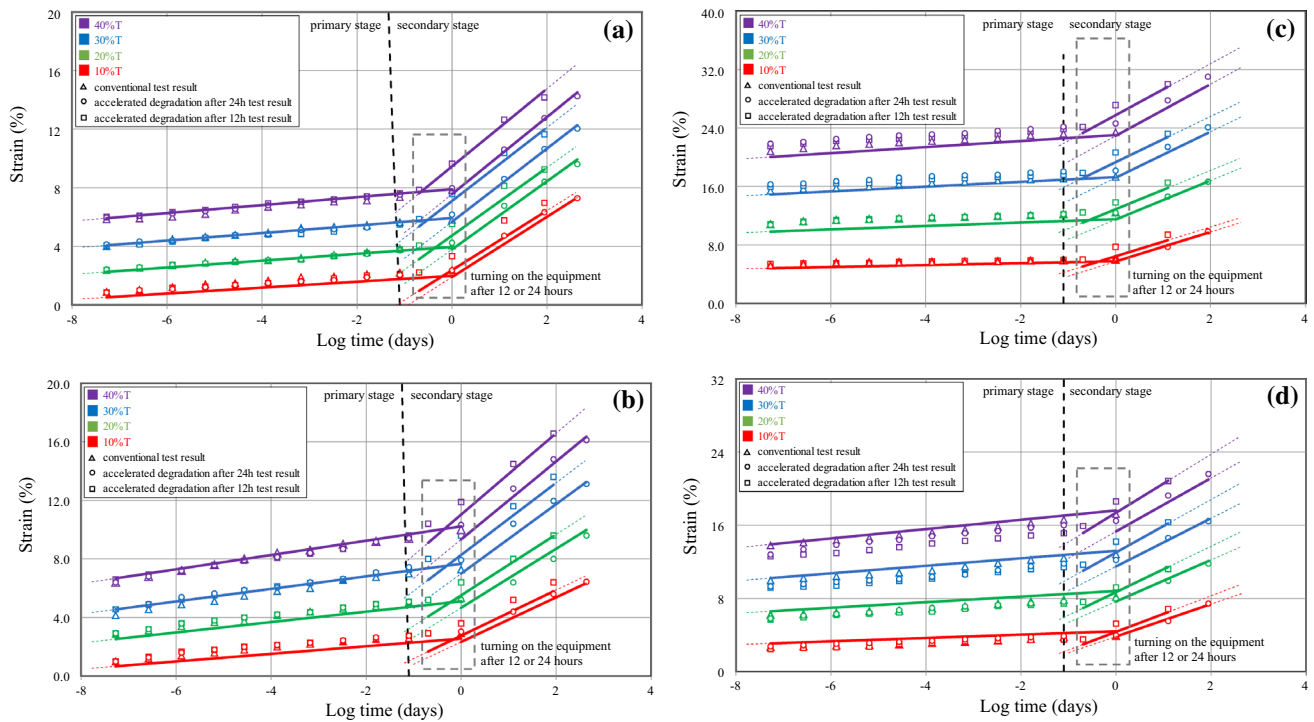
Fig. 7 Comparison between the experimental data and the extrapolation model for the accelerated creep deformation tests at four loading levels for each geotextile tested: **a** PET340; **b** PP500; **c** PET740; **d** PP925

degradation with a marked increase in the deformation rate over time for the four load levels applied.

The slopes relating to saturation and drying showed a high deformation rate that reached values close to rupture. According to Dias Filho et al. [40], it is possible to generate models with these data to estimate the deformations during the beginning of the test with the parameters obtained from the curves and which are shown in Table 2.

Based on the creep parameters, it was possible to assess the consistency of both the conventional creep data and the accelerated tests, which are indicated by the model. It is

evident that there is little variation between the trends generated by the coefficients of determination (R^2). The correlations between these data were generated and are presented in Table 3. Most of creep curves for the samples show little scatter ($R^2 > 0.973$). The first battery of conventional creep tests for PET340, even with an R^2 around 0.85, showed good correlation between experimental and modeling data collected for each load.

To determine the durability of the geotextiles based on creep test and load levels varying between 50 and 90%, extrapolation of the data was done using the models

Table 2 Coefficient statistics creep curve parameters calculated from experimental data collected over time for each geotextile tested

Parameter		PET340	PP500	PET740	PP925
Conventional test (M/CV)	c	(0.140/3.9)	(0.088/1.7)	(0.014/4.5)	(0.024/3.2)
	d	(0.219/6.4)	(0.457/1.2)	(0.826/3.0)	(0.740/1.4)
	e	(0.376/0.3)	(0.241/0.9)	(0.382/0.9)	(0.284/2.3)
Accelerated test (24 h/12 h)	c	(1.535/1.480)	(0.588/0.584)	(0.675/0.664)	(0.663/0.759)
	d	(0.177/0.192)	(0.403/0.416)	(0.404/0.407)	(0.359/0.348)
	e	(0.360/0.450)	(0.220/0.260)	(0.380/0.427)	(0.247/0.280)
Tensile load (T—kN/m)	10%T	5.25	10.60	15.07	15.50
	20%T	10.50	21.20	30.14	31.00
	30%T	15.75	31.80	45.21	46.50
	40%T	21.00	42.40	60.28	62.00

M mean, *CV* coefficient of variation in %, *c* multiplication coefficient (%/T^d), *d* dimensionless power of the power behavior, *e* slope coefficient (%/kN/m)

Table 3 Coefficient of determination between experimental and modeling data collected for each load level of the geotextiles tested

Geotextiles	Load level	Conventional test	Non-conventional test	
			24 h	12 h
PET340	10%T	0.847	0.996	0.996
	20%T	0.843	0.998	0.994
	30%T	0.845	1.000	0.995
	40%T	0.849	1.000	0.997
PP500	10%T	0.999	1.000	0.998
	20%T	0.999	0.986	0.999
	30%T	0.997	0.998	0.999
	40%T	0.998	0.999	1.000
PET740	10%T	0.973	0.990	0.991
	20%T	0.998	0.999	0.998
	30%T	0.996	1.000	0.988
	40%T	0.995	0.997	0.990
PP925	10%T	0.992	0.991	0.989
	20%T	0.995	0.998	0.998
	30%T	0.997	1.000	0.984
	40%T	0.997	1.000	0.984

generated by the creep equations for loads of 10, 20, 30 and 40% of the rupture load of the studied materials. The criterion used to define the rupture event was the elongation at rupture. The value was obtained with Eq. 1, based on the elongation at rupture determined from the wide-width strip test, to assess the limits at which the results could be reached without conservative data.

Figure 8 shows the trend generated by the rupture data derived from the model, the equations and coefficients of determination. As can be seen, the significant variation in the tensile strength over time can be evaluated based on the weight and base polymer of the geotextiles. Based on 50% of

rupture load, PET340 and PP500 exceed 1000 years before reaching failure. Whereas the PP925 geotextile reached a value of 982 years and the PET740 reached 337 years. In fact, similar durability was expected for the materials with the same polymer. This highlights a limitation related to the constructed equipment, which was the difficulty of manually applying loads greater than 10 kg to the PET740 and PP925 test levers. An automatic system or load application control over the first minute may be a future solution to this problem.

Using the test results, several reduction factors were calculated. The aim was to compare the influence over the years for the creep durability prediction. The creep reduction factor was determined as the inverse of the tensile strength of each sample. The most conservative value for 10 years of service time was 1.91 for the PET740 sample, while the PET340 sample yielded a value of 1.40.

Similarly, Fig. 9 presents results of the rupture model and durability prediction method using data from the accelerated degradation procedure based on the test data reflected in the secondary stage of the curve after the saturation-drying equipment was turned on and higher deformation rates occurred.

As can be seen, some reduction factor values for 2, 5 and 10 years are not presented. The time scale for the accelerated test was not representative, because the degradation process was very accelerated. The results enabled evaluations over time for up to 5 years. The predictions of the creep rupture response after degradation using the results seem to be unsafe, with reduction factors greater than 3. In the case of sample PP925, for example, the accelerated creep reduction factor was 2.2 times greater than the conventional creep test result at just 3 months and reaching 14.5 times for 5 years.

The extrapolations from the predictions of accelerated creep rupture resulted in a useful life of less than 1 year of use for material under 50% of rupture load. Koerner and

Fig. 8 Rupture model and conventional creep durability prediction for each geotextile tested
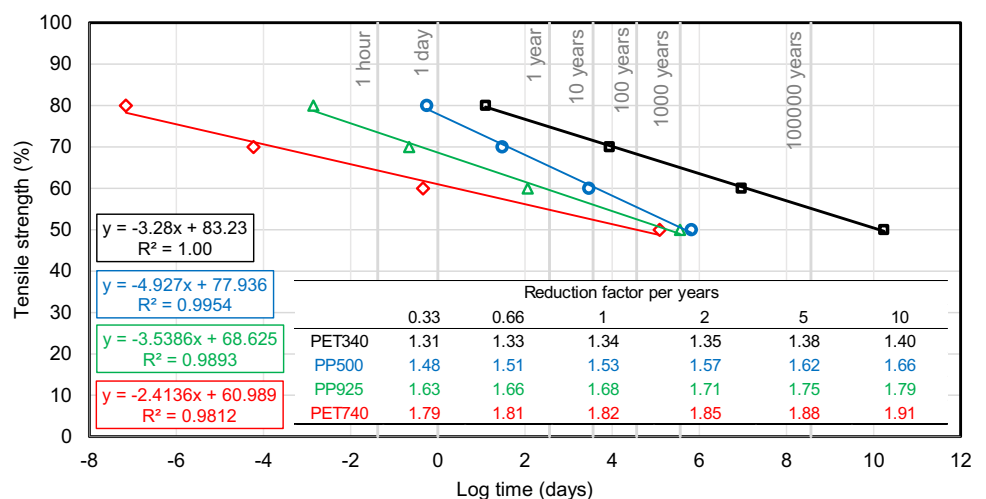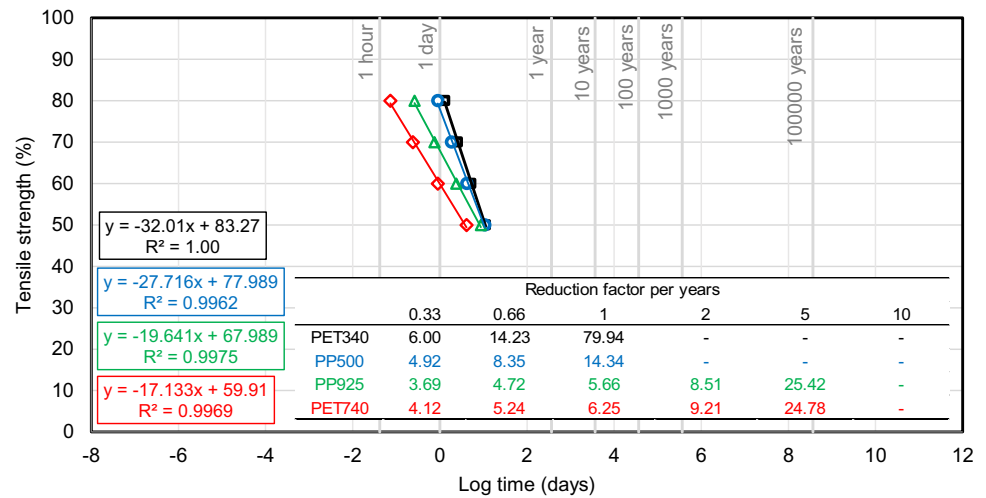
Fig. 9 Rupture model and accelerated creep durability prediction for each geotextile tested

The figure contains the following fitted equations:

$$y = -32.01x + 83.27 \quad R^2 = 1.00$$
$$y = -27.716x + 77.989 \quad R^2 = 0.9962$$
$$y = -19.641x + 67.989 \quad R^2 = 0.9975$$
$$y = -17.133x + 59.91 \quad R^2 = 0.9969$$

Axes: Tensile strength (%) versus Log time (days)

Reduction factor per years						
	0.33	0.66	1	2	5	10
PET340	6.00	14.23	79.94	-	-	-
PP500	4.92	8.35	14.34	-	-	-
PP925	3.69	4.72	5.66	8.51	25.42	-
PET740	4.12	5.24	6.25	9.21	24.78	-

Koerner [21] presented temperature monitoring in their database for the geosynthetic studied, where temperature conditions varied between 20 and 45 °C with a temperature gradient of approximately 25 °C. Regarding the values used in the present study, the equipment temperature limits are between 30 and 70 °C with a gradient of 40 °C. This may explain the sharp increase in deformations under constant load during cycling. This indicates that these materials exhibit a high susceptibility to the degradation procedure, which can be changed with an alteration in the cycling time intervals and temperature gradient.

The micrographs of the materials tested before and after the accelerated creep test are shown in Fig. 10. Only images of the PET340 polyester and PP500 polypropylene materials are provided, as they similarly characterize the surface of the two polymer bases of the analyzed geotextiles. In comparing the micrographs of the degraded material with the intact one, the surfaces of the both polymers exhibited higher density relative to surface roughness. The PP laminates also revealed parallel superficial micro-cracks, with linear patterns and a decrease in the number of loose fibers. These micrographs demonstrate that degradation by saturation and drying cycles in geotextiles generated the observed changes. Therefore, it is to be expected that these changes have influenced the behavior of the increase in deformation after the accelerated degradation procedure.

Conclusions

This paper focused on the long-term performance and service life of geosynthetics by comparing laboratory results from conventional creep tests to a non-conventional test procedure. To better approximate exogenous field conditions, a test was developed to simulate creep under accelerated conditions using a saturation and drying procedure simultaneous to the creep process. Thus, four woven geotextiles were characterized by means of 48 creep tests, and a methodology applied to the data provided a direct parameter of durability.

From the results, there are a number of main conclusions.

- The methodology for creation of creep curve models got coefficients of determination greater than 0.84. In addition, extrapolations were generated to predict the deformation by combination of creep and saturation and drying cycles of structures designed for the woven geotextiles yielding estimates exceeding 300 years, with reduction factors ranging between 1.50 and 2.05.
- After simulate creep under accelerated conditions, the potential for creep rupture decreased when compared to conventional creep test. The accelerated conditions increased the strain during the creep test reflecting in a reduction factor ranging between 3.69 and 80, which would make it impractical to design structures with these geotextiles. Evaluations were limited to projections of up to 5 years. The low predicted life expectancies are not representative.
- The test equipment can be reconfigured to better characterize the exogenous geotextile exposure environment, thereby representing results in accordance with the susceptibility to degradation, as well as the intensity of the degradation agent, and, consequently, better represent any environment for the application of geosynthetics. The time and temperature variables used for the equipment cycles should be better studied to conduct more tests and better understand the behavior of the materials studied.
- The long-term response of the four geotextiles were affected by saturation and drying cycles. The changes in mechanical response observed could be related to the visual changes observed by the micrographs due alterations in the geotextiles after the accelerated degradation procedure.

Fig. 10 Micrographs of geo-textile samples before and after the accelerated degradation procedure: **a** intact polyester; **b** degraded polyester; **c** intact polypropylene; **d** degraded polypropylene
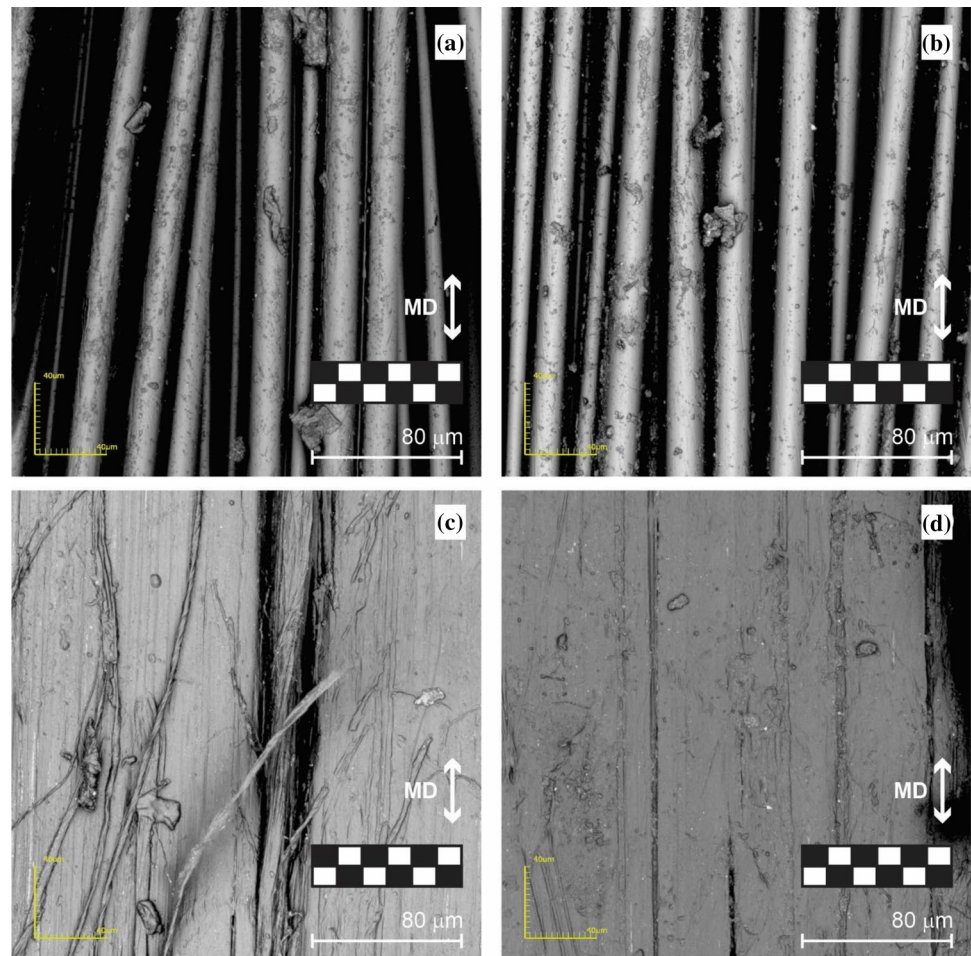
As the creep behavior of geosynthetics may lead to failure of a geosynthetic application, it is essential to realistically estimate the influence of simultaneous degradation. The results from these accelerated degradation tests yielded high reduction factors indicating that current design approaches could be unsafe for geotextiles under the test conditions considered in this paper. It is important to highlight that the proposed accelerated degradation procedure should be studied further.

Availability of data and material All data, models, and code generated or used during the study appear in the published article.

Code availability Not applicable.

Declarations

Conflict of interest Not applicable.

Ethics approval Not applicable.

Additional declarations for articles in life science journals that report the results of studies involving humans and/or animals Not applicable.

Consent to participate Not applicable.

Consent for publication Not applicable.

References

1. Suits LD, Hsuan YG (2003) Assessing the photo-degradation of geosynthetics by outdoor exposure and laboratory weatherometer. Geotext Geomembr 21(2):111–122. https://doi.org/10.1016/S0266-1144(02)00068-7

2. Guimarães MGA, Urashima DC, Vidal DM (2014) Dewatering of sludge from a water treatment plant in geotextile closed systems. Geosynth Int 21(5):310–320. https://doi.org/10.1680/gein.14.00018

3. Koerner RM, Hsuan YG, Koerner GR (2017) Lifetime predictions of exposed geotextiles and geomembranes. Geosynth Int 24(2):198–212. https://doi.org/10.1680/jgein.16.00026

4. Carneiro JR, Morais M, Lopes ML (2018) Degradation of polypropylene geotextiles with different chemical stabilisations in marine environments. Constr Build Mater 165:877–886. https://doi.org/10.1016/j.conbuildmat.2018.01.067

5. Dias Filho JLE, Maia PCA, Xavier GDC (2019) Spectrophotometry as a tool for characterizing durability of woven geotextiles. Geotext Geomembr 47(4):577–585. https://doi.org/10.1016/j.geotexmem.2019.02.002

6. Sehgal CK (1996) Design guidelines for spillway gates. J Hydraul Eng 122(3):155–165. https://doi.org/10.1061/(ASCE)0733-9429(1996)122:3(155)

7. Koffler A, Choura M, Bendriss A, Zengerink E (2008) Geosynthetics in protection against erosion for river and coastal banks and marine and hydraulic construction. J Coast Conserv 12(1):11–17. https://doi.org/10.1007/s11852-008-0023-x

8. Restall SJ, Jackson LA, Heerten G, Hornsey WP (2002) Case studies showing the growth and development of geotextile sand containers: an Australian perspective. Geotext Geomembr 20(5):321–342. https://doi.org/10.1016/S0266-1144(02)00030-4

9. Hornsey WP, Carley JT, Coghlan IR, Cox RJ (2011) Geotextile sand container shoreline protection systems: design and application. Geotext Geomembr 29(4):425–439. https://doi.org/10.1016/j.geotexmem.2011.01.009

10. Kim HJ, Park TW, Dinoy PR, Kim HS (2021) Performance and design of modified geotextile tubes during filling and consolidation. Geosynth Int 28(2):125–143. https://doi.org/10.1680/jgein.20.00035

11. Alvarez E, Rubio R, Ricalde H (2007) Beach restoration with geotextile tubes as submerged breakwaters in Yucatan, Mexico. Geotext Geomembr 25(4):233–241

12. Shin EC, Oh YI (2007) Coastal erosion prevention by geotextile tube technology. Geotext Geomembr 25(4):264–277. https://doi.org/10.1016/j.geotexmem.2007.02.005

13. Dias Filho JLE, Maia PCA, Xavier GC, Corrêa BRF (2016) CBR test in geosynthetics with confined support using sands. Eletron J Geotech Eng 21(5):1681–1689

14. Cheng H, Yamamoto H, Thoeni K, Wu Y (2017) An analytical solution for geotextile-wrapped soil based on insights from DEM analysis. Geotext Geomembr 45(4):361–376. https://doi.org/10.1016/j.geotexmem.2017.05.001

15. Pinho-Lopes M, Paula AM, Lopes MDL (2018) Long-term response and design of two geosynthetics: effect of field installation damage. Geosynth Int 25(1):98–117. https://doi.org/10.1680/jgein.17.00036

16. Carlos DM, Carneiro JR, Lopes MDL (2019) Effect of different aggregates on the mechanical damage suffered by geotextiles. Materials 12(24):4229. https://doi.org/10.3390/ma12244229

17. Almeida F, Carlos DM, Carneiro JR, Lopes MDL (2019) Resistance of geosynthetics against the isolated and combined effect of mechanical damage under repeated loading and abrasion. Materials 12(21):3558. https://doi.org/10.3390/ma12213558

18. Elias T, Shirlal KG, Kajal EV (2021) Physical model studies on damage and stability analysis of breakwaters armoured with geotextile sand containers. Geotext Geomembr 49(3):604–618. https://doi.org/10.1016/j.geotexmem.2020.12.001

19. Tan X, Hu Z, Cao M, Chen C (2020) 3D discrete element simulation of a geotextile-encased stone column under uniaxial compression testing. Comput Geotech 126:103769. https://doi.org/10.1016/j.compgeo.2020.103769

20. Koerner RM, Hsuan YG, Koerner GR, Gryger D (2010) Ten year creep puncture study of HDPE geomembranes protected by needle-punched nonwoven geotextiles. Geotext Geomembr 28(6):503–513. https://doi.org/10.1016/j.geotexmem.2009.12.014

21. Rowe RK, Hamdan S (2021) Effect of wet-dry cycles on standard & polymer-amended GCLs in covers subjected to flow over the GCL. Geotext Geomembr. https://doi.org/10.1016/j.geotexmem.2021.03.010

22. Prellwitz MF, Maia PCA, Dias Filho JLE (2014) Influence of drying temperature on punching resistance in geotextile fabrics through wet and dry degradation test. In: Proceedings of the 10th international conference on geosynthetics, Berlin

23. Rowe RK, Bostwick LE, Take WA (2011) Effect of GCL properties on shrinkage when subjected to wet-dry cycles. J Geotech Geoenviron Eng 137(11):1019–1027. https://doi.org/10.1061/(ASCE)GT.1943-5606.0000522

24. Kongkitkul W, Tatsuoka F, Hirakawa D (2007) Creep rupture curve for simultaneous creep deformation and degradation of geosynthetic reinforcement. Geosynth Int 14(4):189–200. https://doi.org/10.1680/gein.2007.14.4.189

25. Perkins SW (2000) Constitutive modeling of geosynthetics. Geotext Geomembr 18(5):273–292. https://doi.org/10.1016/S0266-1144(99)00021-7

26. Cantré S, Saathoff F (2011) Design method for geotextile tubes considering strain - Formulation and verification by laboratory tests using photogrammetry. Geotext Geomembr 29(3):201–210. https://doi.org/10.1016/j.geotexmem.2010.10.009

27. Guimarães MGA, Vidal DM, Urashima DC, Castro CAC (2017) Degradation of polypropylene woven geotextile: tensile creep and weathering. Geosynth Int 24(2):213–223. https://doi.org/10.1680/jgein.16.00029

28. ISO/TS 13434 (2008) Geosynthetics—guidelines for the assessment of durability. International Organization for Standardization, Brussels, Belgium

29. ASTM D5970, D5970M-16 (2021) Standard test method for deterioration of geotextiles from outdoor exposure. American Society for Testing and Materials, West Conshohocken

30. ASTM G90 (2010) Standard practice for performing accelerated outdoor weathering of nonmetallic materials using concentrated natural sunlight. American Society for Testing and Materials, West Conshohocken

31. ASTM D5819 (2005) Standard guide for selecting test methods for experimental evaluation of geosynthetic durability. American Society for Testing and Materials, West Conshohocken

32. Carneiro JR, Almeida PJ, Lopes ML (2014) Some synergisms in the laboratory degradation of a polypropylene geotextile. Constr Build Mater 73:586–591. https://doi.org/10.1016/j.conbuildmat.2014.10.001

33. Carneiro JR, Almeida PJ, Lopes ML (2018) Laboratory evaluation of interactions in the degradation of a polypropylene geotextile in marine environments. Adv Mater Sci Eng. https://doi.org/10.1155/2018/9182658

34. Carneiro JR, Lopes ML (2017) Natural weathering of polypropylene geotextiles treated with different chemical stabilisers. Geosynth Int 24(6):544–553. https://doi.org/10.1680/jgein.17.00020

35. Guimarães MGA, Urashima DC, Castro CAC, Lopes MLC (2015) Durability of a polypropylene woven geotextile under climatic and

chemical agents. Modern Environ Sci Eng 1(4):172–177. https://doi.org/10.15341/mese(2333-2581)/04.01.2015/002

36. ASTM D5035-11 (2015) Standard test method for breaking force and elongation of textile fabrics (strip method). ASTM, West Conshohocken

37. ASTM D5261 (2010) Standard test method for measuring mass per unit area of geotextiles. ASTM, West Conshohocken

38. ASTM D5199 (2012) Standard test method for measuring the nominal thickness of geosynthetics. ASTM, West Conshohocken

39. ASTM D5262 (2007) Standard test method for evaluating the unconfined tension creep and creep rupture behavior of geosynthetics. ASTM, West Conshohocken

40. Dias Filho JLE, Maia PCA, Xavier GDC (2019) A short-term model for extrapolating unconfined creep deformation data for woven geotextiles. Geotext Geomembr 47(6):792–797. https://doi.org/10.1016/j.geotexmem.2019.103492